DELPHI 97-85 CONF 71
28 July, 1997

Updated results on the energy dependence of the differences between the quark and gluon jet fragmentation

Preliminary

DELPHI Collaboration

R. Alemany[a], C. García[a], S. Cabrera[a], J. Fuster[a] and S. Martí i García[b]
a) IFIC, Avda. Dr. Moliner 50, E-46100 Burjassot-València, Spain
b) University of Liverpool, Physics Department, Oliver Lodge laboratory,
Oxford Street, Liverpool L69 7ZE, U.K.

Abstract

The analysis of the data collected by DELPHI during 1994 at the Z^0 peak, has allowed updating the results of the charged multiplicity of quark and gluon jets. The new values confirm the energy dependence of the multiplicity ratio, r, of gluon to quark jets, giving:

$$\frac{\Delta r}{\Delta E} = (0.0112 \pm 0.0024)\ GeV^{-1}$$

As a consequence of the energy dependence exhibited by the jet multiplicities, b quark and gluon initiated jets of 25 GeV manifest similar properties.

The study of the string effect, by means of the particle flow in the $q\bar{q}$ inter-jet region of the $q\bar{q}g$ and $q\bar{q}\gamma$ events, confirms with increased accuracy the perturbative QCD calculation.

Paper submitted to the LP'97 Conference
Hamburg, July 28 - August 1st

1 Introduction

The colour dynamics confers different colour charges to quarks and gluons. As gluons carry colour charge, they can interact among themselves (e.g. triple-gluon vertex). Therefore, gluons experience a hadronization process similar to the one for quarks. At the end of this process, the remaining particles are colourless hadrons. These particles emerge in the event forming jets. In a $e^+e^- \to q\bar{q}$ event with two hadronic jets in the final state, the direction of the jets matches that of the primary quarks [1]. Thus, the jet structure of the event (their energy and direction) is a record of the earliest stage of the hadronic process, when the interacting particles are the primary quarks and gluons, and a consequence of colour dynamics at small distances. Thus a $e^+e^- \to q\bar{q}g$ event with a hard bremsstrahlung gluon will manifest a three jet structure at hadron level.

The hadron jets contain information about their originating particle. Consequently in a b quark initiated jet, it is expected to find remains of the long lived B messons and signs of their decays, such as secondary vertices, or presence of leptons. For the gluon jets, large multiplicity could be considered as a sign of its gluonic origin. According to the colour factors of the gluon-gluon and quark-gluon coupling (in SU(3): $C_A = 3$ and $C_F = 4/3$), the naïve expectation for the multiplicity ratio of gluon to quark jets is 9/4. However the hadronization effects introduce large corrections to this expectation. That is well reflected in the experimental results as values close to 1.2 are obtained [2, 3, 4, 5]. The size of the hadronization effects are bigger at low energy, where α_s becomes quite large [4, 5]. At high energies α_s decreases, thus the experimental value of the multiplicity ratio ($1.4 \sim 1.5$) becomes closer to the naïve expectation [5, 6].

The dependence of the hadronic multiplicity on the the center of mass energy is well established theoretically [7] and experimentally [5, 8, 9]. In the same sense, the multiplicity of both quark and gluon jets should depend on the jet energy. This effect has been investigated using Monte Carlo event generators (JETSET and HERWIG in references [10, 6] respectively), and experimentally by DELPHI [5, 11]. The gluon jet multiplicity grows faster with the energy than quark jet multiplicity does, therefrom the multiplicity ratio increases with the energy. Moreover this fact is related with the different scaling violations occurring in quark and gluon jet splitting [12].

It is also true that the jet energy is not the only factor that determines the multiplicity of quark and gluon jets [13], especially if gluon jets are found in $e^+e^- \to q\bar{q}g$ giving three-jet events. The strength of the colour field connecting these particles depends on the relative orientation between them. In order to determine the possible effects of the relative jet orientation on the multiplicity, the string effect [14, 5] and the dependence of the multiplicity with the proper jet scale provide valuable information [13].

The aim of this note is to update the published results by DELPHI on the *energy dependence of the differences between the quark and gluon jet fragmentation* [5]. A similar analysis to the one already published is repeated with data collected by DELPHI during 1994. About 1.4 million Z^0 hadronic decays are now included, thus improving the whole statistics. The gluon jets were extracted from three-jet hadronic Z^0 decays (referred as $q\bar{q}g$-like events), where two jets are tagged as heavy quark initiated jets, while the remaining jet was taken as the gluon jet. An unbiased sample of quark jets is selected from a sample of $q\bar{q}\gamma$ events, where the γ replaces the gluon preserving the same kinematics. The interested reader can found the exact details of the analysis in the references [5, 15].

2 The DELPHI detector

The DELPHI detector is described in detail in reference [16] and its performance in [17]. A brief description of those parts of DELPHI most relevant to this analysis is presented here.

The barrel region of DELPHI contains the superconducting solenoidal coil providing a uniform magnetic field of 1.23 T parallel to the beam direction. The central tracking detectors (vertex detector, inner detector, time projection chamber and outer detector) provide measurements in three dimensions of the tracks of charged particles. The vertex detector consists in three concentric layers of silicon microstrip detectors. In 1994 this detector was upgraded and two of the layers were replaced by double sided silicon microstrip detectors. The inner detector was a cylindrical jet chamber surrounded by five layers of multi-wire proportional chambers. The time projection chamber is the main tracking device, that also provides information on energy loss, dE/dx. The tracking in the barrel region is completed by the outer detector which is composed of five layers of drift cells. The DELPHI tracking system provides an average momentum resolution of $\sigma(p)/p = 3.6\%$ for muons of 45 GeV/c.

The electromagnetic calorimetry is accomplished by the HPC and FEMC (in the barrel and forward region respectively). Their information will allow identifying electrons and photons. The muon identification is performed with the muon detector system, located within and beyond the outer layers of the hadron calorimeter (HCAL).

3 Analysis Method

3.1 Event selection

In the previous publication [5], the data collected by DELPHI through the years 1992 to 1993 were considered. In this update, the data recorded during 1994 are analyzed, and the obtained results will be combined with those already published.

3.1.1 $q\bar{q}g$-like event selection

The three-jet hadronic event selection works as follows:

- first: a quality cut is imposed to all charged tracks and neutral clusters reconstructed by DELPHI. Identified electron-positron pairs arising from photon conversions were replaced by their originating photons.

- second: the hadronic event selection is performed by demanding a minimum charged multiplicity, enough visible energy, and event well contained within the detector volume, with a veto on events containing mismeasured charged or neutral particles. The number of events satisfying these criteria in the 1994 data set is approximately 1.4 million.

- third: charged and neutral particles were grouped into jets by means of the Durham jet finding algorithm ($y_{cut} = 0.01$) [18]. Only those events reconstructed with three jets were considered. Further quality cuts were applied on each jet by requiring a minimum charged multiplicity, enough visible energy and jet direction contained in the barrel part of DELPHI. In addition, only those events with a planar configuration were retained.

Those events satisfying these three-jet event selection criteria formed the $q\bar{q}g$-like sample. The event statistics are quoted in table 1. The estimated background from non-hadronic events in the $q\bar{q}g$ sample was negligible.

Table 1: Number of selected events in the analyzed data sample.

event selection	1994 data analysis	Previous publication[5]
$q\bar{q}g$	316857	319095
$q\bar{q}\gamma$	1015	1012

3.1.2 $q\bar{q}\gamma$-like event selection

Radiative $q\bar{q}\gamma$ events were used to select an unbiased sample of quark jets. The selection process is similar to the one for $q\bar{q}g$-like events. However the presence of a jet formed only by an isolated photon was required. In order to achieve a high purity for the photon sample, a minimum isolation angle of 20° degrees w.r.t. any charged particle of the event and a minimum reconstructed energy of 5 GeV were required (see figure 1). The two quark jets of each selected event were used in the analysis. The energy spectrum of the selected quark jets is presented in figure 2.

The statistics of $q\bar{q}\gamma$ events are presented in table 1. The background arises mainly from two sources: misidentified π^0 represented a 8.7% and the $\tau^+\tau^-\gamma$ the 2.6% of the events.

The different coupling of each quark flavour to the γ and the Z^0 influences on the flavour composition of the $q\bar{q}\gamma$ events. By selecting $q\bar{q}\gamma$ events, the sample is mainly composed of light quarks. The contents on c and b flavour are approximately 33% and 11% respectively.

3.2 Jet energy

The true energy of each jet was derived from the angles between the jet directions:

$$E_j^{calc} = \frac{\sin\theta_j}{\sin\theta_1 + \sin\theta_2 + \sin\theta_3}\sqrt{s}, \quad j = 1, 2, 3 \tag{1}$$

where θ_j is the angle formed by the two opposite jets. This E_j^{calc} gave a better representation of the true energy of the jet, than the reconstructed energy by the detector does. The correction to the gluon jet energy due to mass effects in the case of $b\bar{b}g$ events was estimated to be less than 3% in all cases. Since now, all references to the jet energy (E_j) will mean calculated jet energy (E_j^{calc}) as derived from formula 1. Quark and gluon jets were grouped into 5 GeV energy bins, covering a range from 7.5 GeV up to 42.5 GeV.

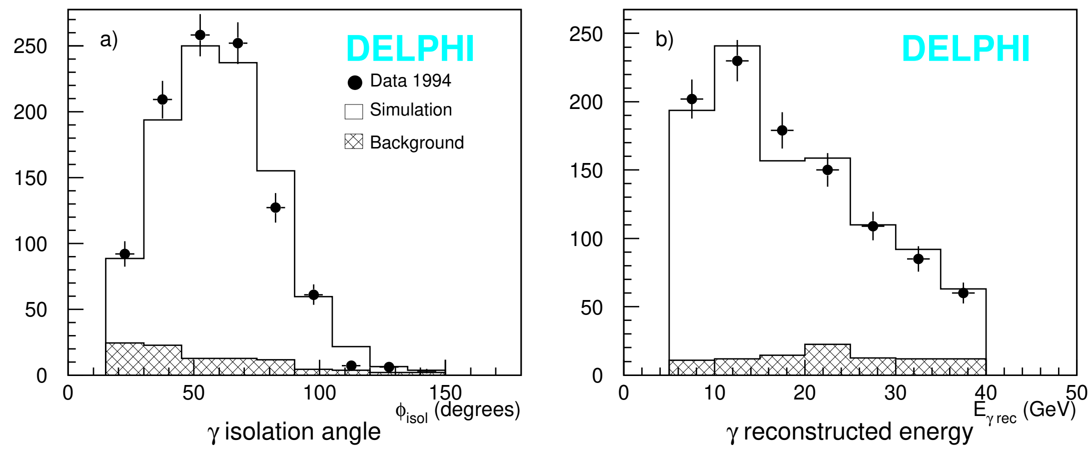

Figure 1: Comparison between real data and Monte Carlo of the isolation angle and reconstructed energy of the photon candidates in the $q\bar{q}\gamma$ sample for 1994 data. Dots represent the real data, solid lines the simulated events, and the dashed are represents the background as estimated from the simulation.

3.3 Identification of gluon jets

In the gluon splitting process ($g \to q\bar{q}$), the heavy quark production is strongly suppressed [19, 20, 21]. Therefore gluon jets can be identified in $b\bar{b}g$ ($c\bar{c}g$) events by tagging two b (c) jets. The techniques for tagging b (c) jets benefit from the fact that the decay products of long lived B (D) hadrons have a large impact parameter and/or contain inclusive high momentum leptons from their semileptonic decays. According to this, the gluon jet identification works as follows:

- **Lepton identification.** Muon candidates were taken from those charged particles with $P \geq 4$ GeV/c detected by the DELPHI muon identification system.

  Electrons were identified by examining the response of the HPC to charged particles and by the energy loss, dE/dx, measured in the TPC. A minimum momentum of 3 GeV/c was required for electron candidates.

  Those events in which one of the two lower energy jets contained a lepton were retained. The most energetic jet and the jet containing the lepton were thus tagged as quark jets, while the remaining jet was considered as gluon jet. These methods will be referred as *muon* and *elec* depending on the lepton used for the tag.

- **Lifetime tag.** In this method a probability function $\mathcal{P}_J$ was constructed for each jet. $\mathcal{P}_J$ represents the probability of containing no decay products from long lived hadrons. The signed impact parameter of each charged particle in each jet was used when evaluating $\mathcal{P}_J$ as derived from the method described in reference [22]. A jet was considered likely to have a secondary vertex if $\mathcal{P}_J < 0.01$. For tagging gluon jets two methods were used.

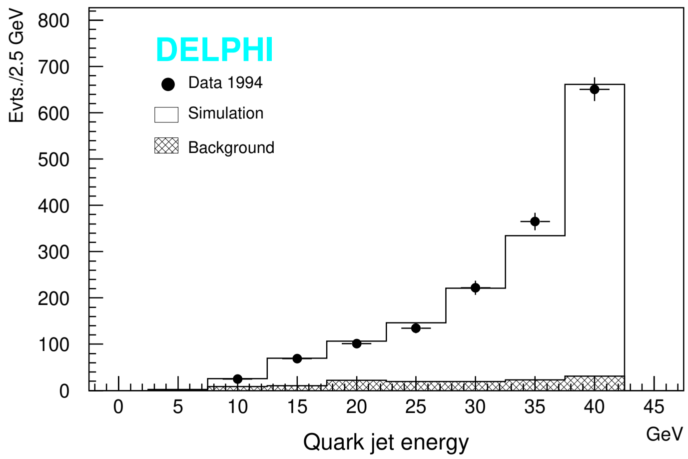

Figure 2: Comparison between real data and Monte Carlo of the energy spectrum of the selected quark jets during 1994.

In the first method, those events in which one of the two lower energy jets had a large probability of having a secondary vertex were considered. The most energetic jet and the jet with $\mathcal{P}_J < 0.01$ were tagged as quark jets, while the remaining jet was tagged as gluon jet. This method will be referred as $1vtx$.

In the second method, those events in which two of the jets had a secondary vertex were labelled as quark jets, while the remaining jet was considered as gluon jet. This method will be referred as $2vtx$.

These gluon jet identification techniques provide us with four samples of gluon jets in a wide energetic range (see figure 3). The event statistics are presented in table 2.

Table 2: Selected gluon jets in 1994 data analysis

	Durham	
method	jets	Purity (%)
muon	8194	74.5
elec	9652	76.0
$1vtx$	35841	82.4
$2vtx$	12810	93.3

3.4 Gluon and quark jet purity

The purity of the selected quark and gluon jet samples were evaluated using the JETSET 7.3 event generator [23], with full simulation of the DELPHI detector. Each simulated

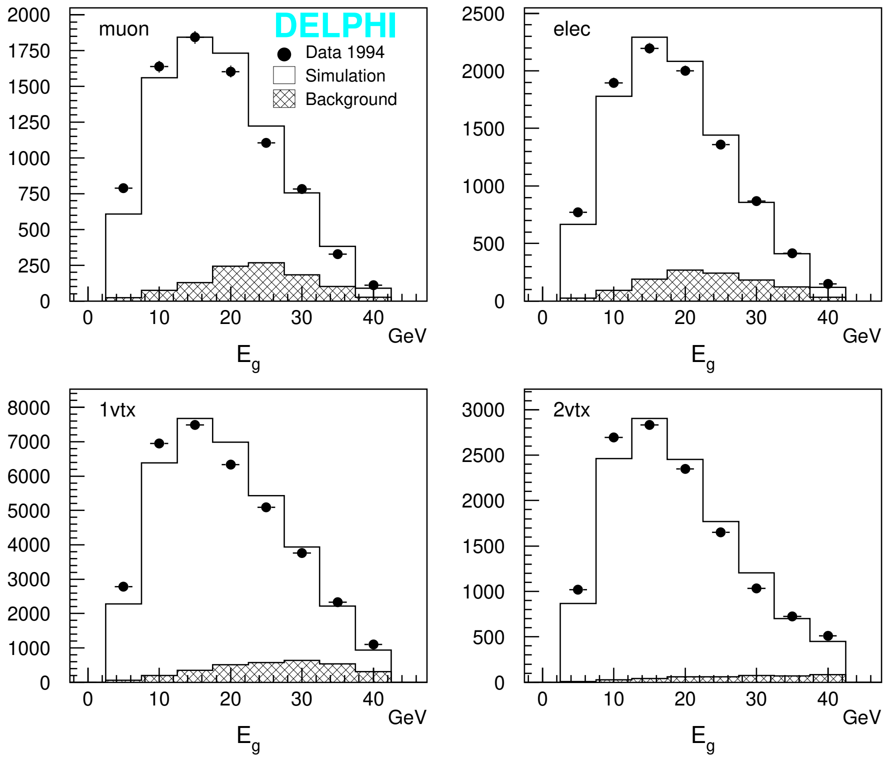

Figure 3: Comparison between the 1994 real data and Monte Carlo of the gluon jet spectrum for the four tagging methods.

event was passed through the same analysis chain than the real data. A total sample of 1.9 million of simulated hadronic events was used.

When estimating the gluon jet purity, each simulated event fulfilling the $q\bar{q}g$ selection criteria (section 3.1.1) at the detector level, was then analyzed at parton level. The parton level jets were built up with the same jet algorithm but choosing the y_{cut} in such a way that three jets were always reconstructed. Then each jet at detector level was associated to the parton level jet that matches better its direction. The two jets at detector level connected with the jets at parton level containing the primary quarks were labelled as quark jets at detector level. Indeed, the third jet, was considered the gluon jet at detector level. The mean purity of each gluon jet tagging method (section 3.3) is presented in table 2. Nevertheless, the purity of each sample is energy dependent (figure 3). To avoid double counting, those gluon jets tagged simultaneously by two methods were only counted once, and included in the categories that gave a better purity.

The purity of the quark jet sample (section 3.1.2) was evaluated using two different samples. The first sample is the already mentioned 1.9 million of hadronic Z decays. This sample was used in order to investigate the misidentified π^0 background. The second sample consisted in 300.000 $\tau^+\tau^-$ events from Z^0 decays generated with KORALZ. None of the $\tau^+\tau^-$ events satisfied the $q\bar{q}g$-like event selection.

4 Quark and gluon jet multiplicity

In this section, the multiplicity of quark and gluon jets are presented as a function of the jet energy. The reconstructed multiplicity, the correction of the detector effects and the multiplicity ratio are detailed.

4.1 Reconstructed charged multiplicity of gluon jets

In order to prove that the techniques of tagging gluon jets do not bias the selected sample, the reconstructed multiplicity of each of the four samples (section 3.3) is presented in figure 4, as a function of the jet energy, and for those points with a purity (P_g) higher than 75%. Indeed it could be seen how the reconstructed multiplicity obtained with each of the four selected samples agree within errors, even without applying any correction.

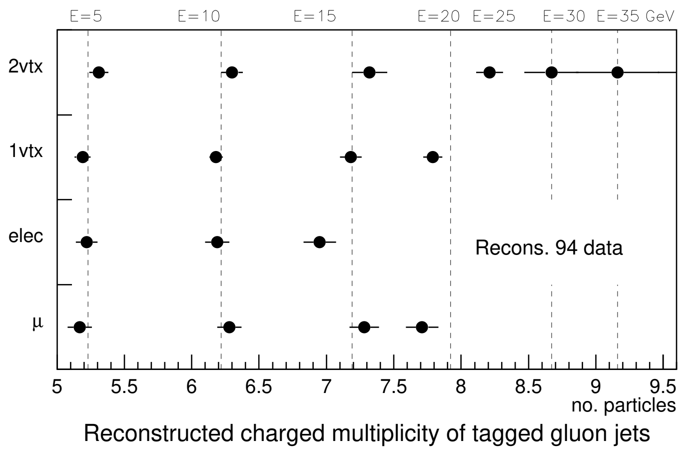

Figure 4: Comparison of the reconstructed charged multiplicity of the tagged gluon jets, for different energies and for those samples with $P_g > 75\%$. Only 1994 data is displayed

4.2 Correction of the detector and tagging effects

The correction of the detector effects accounts for the finite detector resolution for distinguishing two close tracks, inefficiencies, not recorded low momentum particles, acceptance and noise of the associated electronics. Over more, when studying the jet multiplicities, the use of a particular jet finding algorithm has its own effects on the particle association to the different jets in the event [24]. A jet with n_0 charged track has a probability $P(n|n_0)$ of being reconstructed with n. These $P(i|j)$ were use to construct an acceptance matrix, $\mathcal{A}_{ij}$, for each jet type and energy. The $P(i|j)$ were obtained from the simulation of the response of DELPHI to the passage of charged particles. Thus the distribution of the reconstructed charged multiplicity (N^{rec}) is the convolution of the unfolded one (N^{unf}) with the acceptance matrix:

$$N_i^{rec} = \mathcal{A}_{ij} N_j^{unf} \tag{2}$$

The unfolded multiplicity distribution was approximated by a negative binomial distribution (NBD) [25]:

$$P(n:\langle n\rangle, K) = \frac{\Gamma(n+K)}{\Gamma(n+1)\Gamma(K)} \left(1+\frac{K}{\langle n\rangle}\right)^{-n} \left(1+\frac{\langle n\rangle}{K}\right)^{-K} \quad (3)$$

where $P(n:\langle n\rangle, K)$ is the probability to obtain n particles from a NBD with mean $\langle n\rangle$ and broadness K.

For each considered energy interval the parameters of the NBD, $\langle n\rangle$ and K given in formula 3, were fitted according to the following procedure:

- **gluon jet multiplicity:** the four distribution obtained with the tagging techniques ($muon$, $elec$, $1vtx$ and $2vtx$), were fitted simultaneously, keeping the same gluon contribution in the four samples but weighted according to the purity (P_g) derived from the simulation studies, and allowing different background for each sample:

$$N^{rec}_{j,m} = \mathcal{A}_{ij}(P_{g,m}N^{unf}_j + (1-P_{g,m})N^{back}_{j,m}) \qquad m = muon,\ elec,\ 1vtx,\ 2vtx \quad (4)$$

- **quark jet multiplicity:** a similar fit was performed when correcting the quark jet multiplicity, but now a single multiplicity distribution was fitted for each energy bin, taking in account the background in the same way as expressed in formula 4.

4.3 Corrected charged multiplicity of quark and gluon jets

The corrected multiplicities of quark and gluon jets are listed in table 3 and plotted in figure 5.a, where the experimental multiplicities compared with the predicted by JETSET 7.3. It is seen how the quark and gluon jet multiplicity depends on the jet energy. Indeed gluon jet multiplicity is larger than the quark one.

Table 3: Mean charged multiplicity, $\langle n\rangle$, and broadness, K, of gluon and quark jets. Combined result with the 1992, 1993 [5] and the new 1994 data.

E (GeV)	$\langle n_g\rangle$	K_g	$\langle n_q\rangle$	K_q
10	5.79 ± 0.06	23.8 ± 2.9	5.88 ± 0.72	7.6 ± 5.1
15	7.00 ± 0.06	16.9 ± 3.5	5.66 ± 0.31	6.1 ± 2.5
20	8.04 ± 0.09	12.1 ± 2.9	7.43 ± 0.30	5.0 ± 1.8
25	8.97 ± 0.10	10.5 ± 2.4	7.38 ± 0.27	10.7 ± 3.7
30	9.71 ± 0.19	6.5 ± 1.3	7.74 ± 0.30	14.6 ± 5.8
35	10.59 ± 0.30	8.3 ± 1.4	8.26 ± 0.15	12.1 ± 2.8
40	12.40 ± 0.41	5.0 ± 2.1	8.64 ± 0.18	15.1 ± 1.4

The increased precision on the NBD broadness K (arisen since the inclusion of 1994 data with respect to the previous publication [5]) reveals a different trend for K_g and K_q. While K_g decreases with increasing the energy, K_q operates in the opposite sense. Besides, when fitting to NBD's the multiplicity distribution of those quark and gluon jets simulated with JETSET 7.3, the obtained K_g and K_q follow the same behaviour that their counterparts for real data jets.

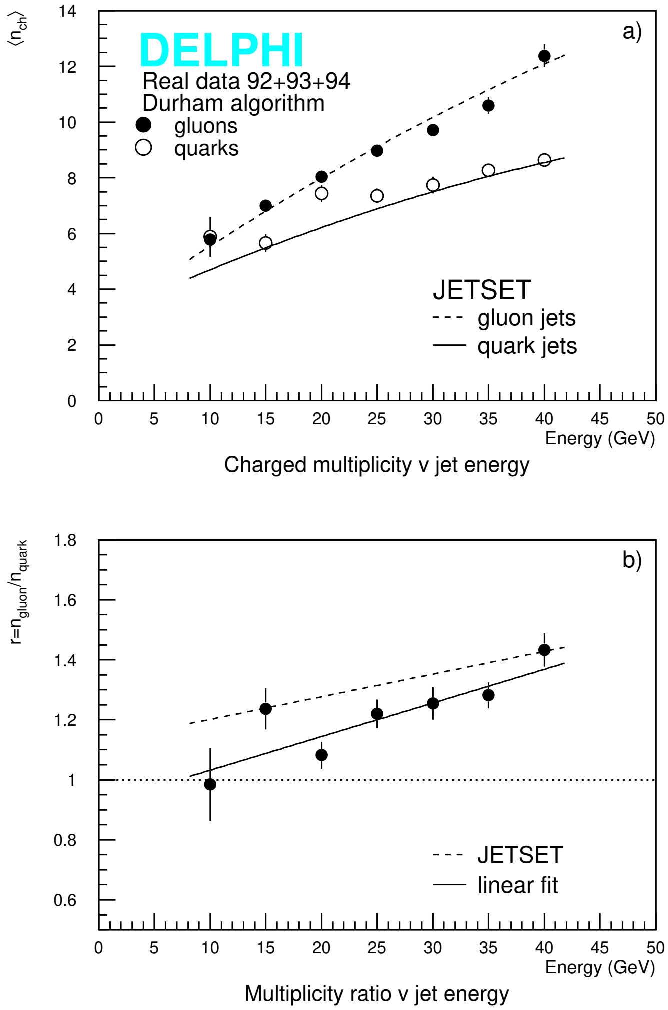

Figure 5: Multiplicity ratio of the quark and gluons jets reconstructed with Durham $y_{cut} = 0.01$, including all analyzed data (1992+93+94).

4.4 Multiplicity ratio

The multiplicity ratio, $r = \langle n_g \rangle / \langle n_q \rangle$, of gluon to quark jets is presented in the figure 5.b. It manifests an increase with the jet energy. In order to estimate the dependence of r with the energy, the simplest functionality that may be considered is a linear dependence. That could be regarded inasmuch as the first order approximation of a much more complex dependence. A fit of r to a straight line gives the following result:

$$r = (0.0112 \pm 0.0024) E(\mathrm{GeV}) + (0.92 \pm 0.07)$$

This result proves the energy dependence of the multiplicity ratio as the slope is not compatible with zero by a 4.7σ effect. It also verifies that quark and gluon jets of very low energy have a similar multiplicity as, $\lim_{E \to 0} \sim 1$.

A comparison of the multiplicity ratio can be made with the results published by CLEO at energies $< 7GeV$ [4] and OPAL at $\sim$ 39 GeV [6]. The CLEO analysis is performed in a different scenario w.r.t the LEP experiments, as CLEO employs the $\Upsilon(1S) \to gg\gamma$ decay and the $e^+e^- \to q\bar{q}\gamma$ events in order to determine the multiplicity ratio of gluon to quark. In this way, CLEO statistics and systematic errors are smaller than ours for quark and gluon jets of 10 GeV. OPAL used a method based on hemisphere analysis. Our results reconcile the values published by CLEO, $r(E < 7GeV) = 1.04 \pm 0.05$, and OPAL, $r(39GeV) = 1.552 \pm 0.073$, as it is proven that r depends on the jet energy.

4.4.1 Effects of the flavour composition

As already mentioned, the flavour composition of the quark jet sample is the one as derived from the quark coupling to the γ and not to the Z^0 (section 3.1.2). In the other hand, it is known that the multiplicity of the $b\bar{b}$ events and $c\bar{c}$ events is larger by $\delta_{bq} = 2.90 \pm 0.33(stat. + syst.)$ and $\delta_{cq} = 1.14 \pm 0.62(stat. + syst.)$ respectively. These excess are seen to be independent of the CM energy [26, 27]. Of course, δ_{bl} together with δ_{cl} and the quark flavour composition affect the jet multiplicity. However the total contribution turned out to be negligible for practical purposes, as the two effect almost compensate each other. The total change of the quark jet multiplicity estimated with the flavour composition corresponding to the γ-quark coupling instead of the Z^0-quark would be approximately +0.06 particles, below our experimental precision (table 3).

Assuming that the multiplicity excess corresponds half to each quark, it is possible to evaluate the charged multiplicity of a 25 GeV b quark jet as:

$$\langle n_b \rangle(25GeV) = \langle n_q \rangle(25GeV) + \frac{\delta_{bq}}{2} = 8.83 \pm 0.44$$

The comparison of $\langle n_b \rangle$ with the multiplicity of gluon jets of the same energy gives:

$$r_b = \frac{\langle n_g \rangle}{\langle n_b \rangle}(25GeV) = 1.02 \pm 0.06$$

in nice agreement with the values published by OPAL and ALEPH [28, 29]. In the OPAL and ALEPH analyses, the b quark and gluon jets of 24 GeV are selected from a three-jet event sample with jets distributed according to the Y-topology (i.e. two-fold symmetric events where the b quark and the gluon jet formed an angle of 150° w.r.t. the most energetic jet), and therefore b quark and gluon jets are compared in a single energy point. The energy dependence of the quark and gluon jet multiplicity and the multiplicity excess of the b events, compared to the light quark events, are at the origin of the similarity between b quark and gluon jets of $24 \sim 25$ GeV, but this does not apply for the entire energy spectrum. In fact the extrapolation of our results predicts: $r_b(E_j < 24GeV) < 1$ and $r_b(E_j > 24Gev) > 1$.

4.5 Dispersion

The most common measure of the width of a distribution is its variance, D: $D^2 \equiv \langle n^2 \rangle - \langle n \rangle^2$. In the case of the NBD (equation 3), D is related with $\langle n \rangle$ and K through:

$$\frac{D^2}{\langle n \rangle^2} = \frac{1}{\langle n \rangle} + \frac{1}{K} \tag{5}$$

Table 4: Ratio of $\langle n \rangle / D$ for quark and gluon jets as derived from equation 5 and the NBD parameters given on table 3.

E (GeV)	$\langle n_g \rangle / D_g$	$\langle n_q \rangle / D_q$
10	2.16 ± 0.04	1.82 ± 0.25
15	2.22 ± 0.09	1.71 ± 0.15
20	2.20 ± 0.12	1.73 ± 0.15
25	2.20 ± 0.19	2.09 ± 0.16
30	1.97 ± 0.12	2.25 ± 0.18
35	2.16 ± 0.11	2.22 ± 0.12
40	1.89 ± 0.27	2.34 ± 0.05

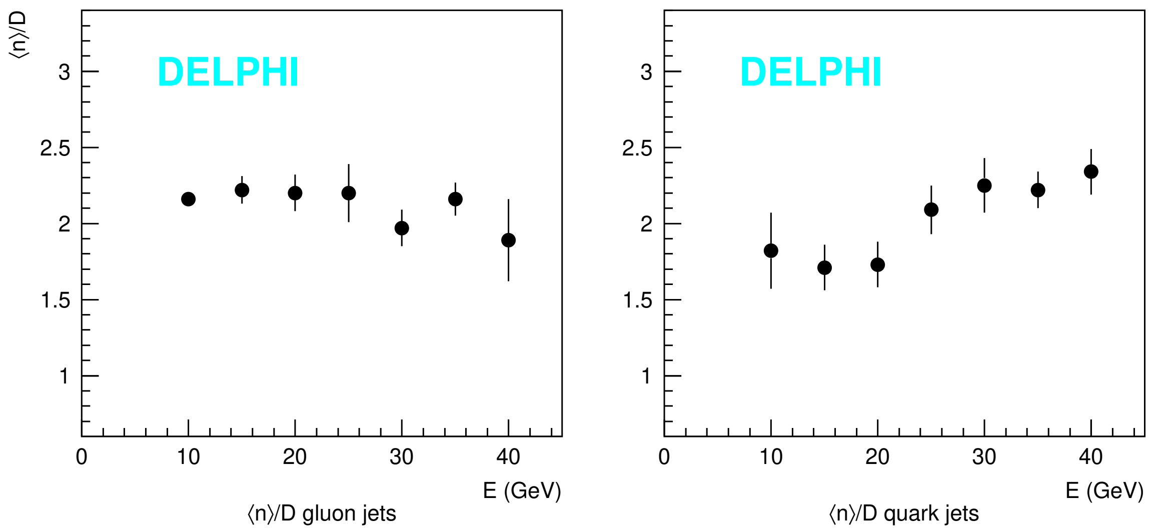

Figure 6: Values of $\langle n \rangle / D$ for gluon (left) and quark (right) jets.

Using the values experimentally obtained for $\langle n \rangle$ and K for quark and gluon jets (table 3), it is possible to calculate the $\langle n \rangle / D$ ratio as presented in table 4 and figure 6.

The behaviour of $\langle n \rangle / D$ for quark and gluon jets is seen to follow a different trend. For gluons, $\langle n \rangle / D$ does not show a strong energy dependence (possible evidence of KNO scaling [30]). However, for quark jets, $\langle n \rangle / D$ grows rapidly with the jet energy. This is just a consequence of the $\langle n \rangle$ and K dependence with the energy (section 4.3 and equation 5). The behaviour exhibited by the real quark and gluon jets is in agreement with those simulated jets with JETSET 7.3 event generator [23]. This is specially true for the simulated quark jets, which $\langle n_q \rangle / D_q$ varies rapidly from ~ 1.9 at 10 GeV to ~ 2.4 at 40 GeV.

5 String Effect

The string effect is a manifestation of the QCD coherence phenomena. Available leading order QCD calculations predicted that the angular distributions of the particle flow in a hadronic three-jet event depends on the colour factors and the topology of the whole jet ensemble as well [14]. The comparison of the particle flow in symmetric $q\bar{q}g$ and $q\bar{q}\gamma$ events allows testing the validity of the perturbative QCD calculation.

Those $q\bar{q}g$ events selected with the $2vtx$ method (section 3.3) with a symmetric jet configuration (i.e. the angle between the two jet quarks, θ_{qq} and the most energetic quark jet and the gluon, θ_{qg} both lying in the interval $150° \pm 10°$) were retained as the $q\bar{q}g$ symmetric events. In the same way, a sample of symmetric $q\bar{q}\gamma$ events (where the γ replaces the g and $\theta_{q\gamma} \sim 150° \pm 10°$) was selected. The total number of events in the symmetric event samples in 1994 data was 1109 and 115 for $q\bar{q}g$ and $q\bar{q}\gamma$ respectively. The particle flow projected to the event plane for those events is presented in figure 7.

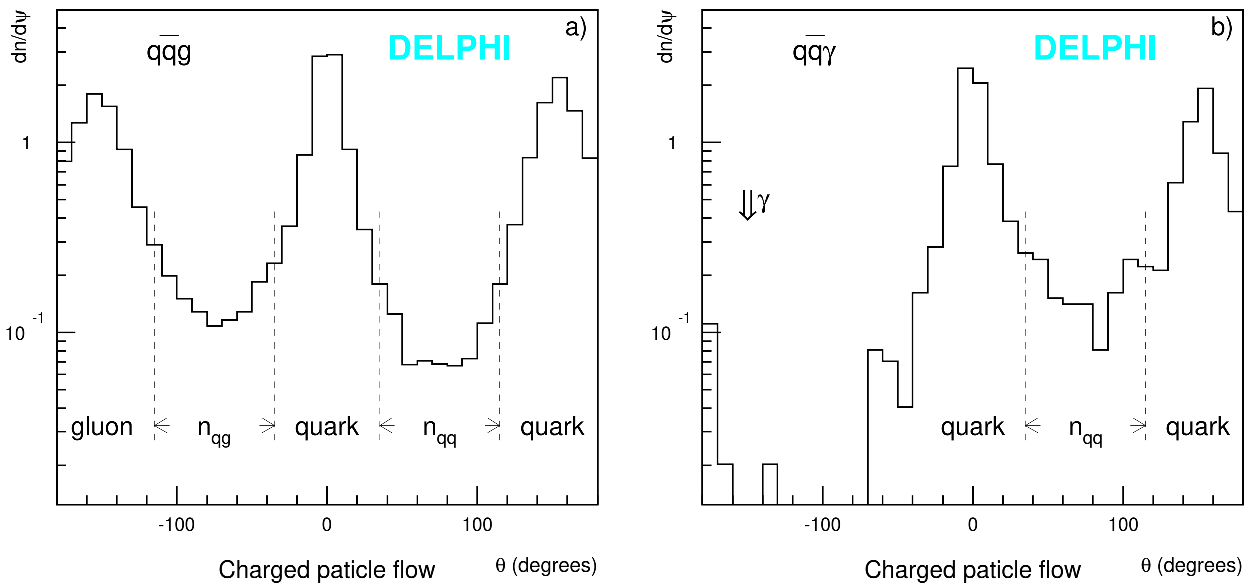

Figure 7: Charged particle flow projected onto the event plane. The angles are measured w.r.t. the most energetic quark jet, and the positive sign is taken in the direction towards the second quark jet. a) $q\bar{q}g$ events. b) $q\bar{q}\gamma$ events. The particle flow is strongly suppressed in the direction of the γ due to the isolation requirements.

The relative particle flow in the interjet region (half angle of the angle defined by two jets, i.e. $\theta/2$) can be approximated by [5]:

$$\frac{N_{q\bar{q}}(q\bar{q}g)}{N_{q\bar{q}}(q\bar{q}\gamma)}(\theta \sim 75°) \approx \frac{0.65n_c^2 - 1}{n_c^2 - 1} \approx 0.60 \qquad (6)$$

where $N_{q\bar{q}}$ represents the particle flow in the corresponding sample and $n_c = 3$ is the number of colours.

The result obtained with DELPHI 1994 data is:

$$\frac{N_{q\bar{q}}(q\bar{q}g)}{N_{q\bar{q}}(q\bar{q}\gamma)}(\theta \sim 75^\circ) = 0.63 \pm 0.05(\text{stat.}) \pm 0.04(\text{syst.})$$

where the systematical error accounts for the corrections due to purity and the jet selection, and the jet definition with Durham.

The combined result with the previously published data by DELPHI [5] is:

$$\frac{N_{q\bar{q}}(q\bar{q}g)}{N_{q\bar{q}}(q\bar{q}\gamma)}(\theta \sim 75^\circ) = 0.61 \pm 0.05(\text{stat.+syst.})$$

in nice agreement with the perturbative QCD calculation given by expression 6.

6 Summary

This note presents the updated results on the energy dependence of quark and gluon jet fragmentation [5] using the data collected by DELPHI during 1994.

The new results from DELPHI confirm the energy dependence of the multiplicity ratio between gluon and quark jets. The increase of $r = \langle n_g \rangle / \langle n_q \rangle$ with energy is:

$$\frac{\Delta r}{\Delta E} = 0.0112 \pm 0.024\text{GeV}^{-1}$$

for the Durham jet definition. Besides, the energy dependence of the multiplicity ratio becomes corroborated when the results from other experiments are included (figure 8), specially those from CLEO at $E_{cm} < 7$ GeV and OPAL at 39 GeV. A linear fit to all points displayed in figure 8.b gives an evidence of 8σ to the energy dependence of the multiplicity ratio, as the following result is obtained:

$$\frac{\Delta r}{\Delta E} = 0.0110 \pm 0.013\text{GeV}^{-1}$$

The energy dependence of the quark and gluon jet multiplicity is the reason why the b quark jet and gluon initiated jets of 25 GeV exhibit a similar multiplicity.

Investigation of the string effect allows testing the perturbative QCD prediction of the $q\bar{q}$ interjet particle flow in $q\bar{q}g$ and $q\bar{q}\gamma$ events. The experimental result is:

$$\frac{N_{q\bar{q}}(q\bar{q}g)}{N_{q\bar{q}}(q\bar{q}\gamma)}(\theta \sim 75^\circ) = 0.61 \pm 0.05(\text{stat.+syst.})$$

in nice agreement within errors with the expected value 0.60 from perturbative QCD calculations.

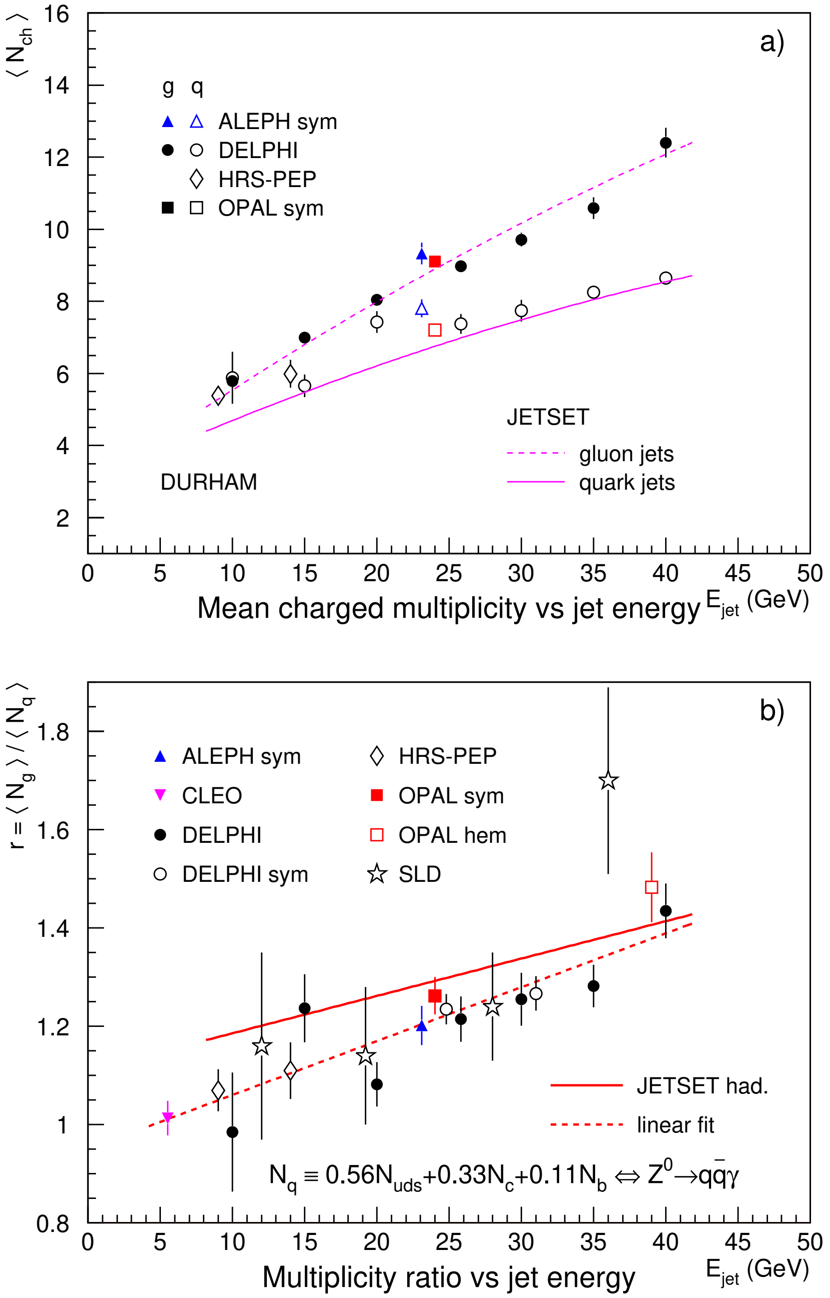

Figure 8: a) Charged multiplicity of quark and gluon jets. b) Multiplicity ratio. Experimental points from other experiments than DELPHI are included for comparison purposes.

References

[1] G. Hanson et al., *Phys. Rev. Lett* ***35*** (75) 1609–1612.

[2] OPAL coll., *Z. Phys. C* ***58*** (93) 387.

[3] ALEPH coll., *Phys. Lett. B* ***346*** (95) 389.

[4] CLEO coll., In *ICHEP 96, Warsaw, Poland*, 1996; ICHEP96 PA04–050, hep–ex/9701006.

[5] DELPHI coll., *Z. Phys. C* ***70*** (96) 179–196.

[6] OPAL coll., *Phys. Lett. B* ***388*** (96) 659-672.

[7] B.R. Webber, *Phys. Lett. B* ***143*** (84) 501–504.

[8] P.V. Chliapnikov et al., *Phys. Lett. B251* (90) 192.

[9] H1 coll., *DESY 96–160, hep–ex/9608011*, 1996.

[10] Z. Fodor, *Phys. Lett. B263* (91) 305.

[11] J. Fuster et al., *QCD 96, Montpellier, France*, 1996; hep–ex/9609004.

[12] DELPHI coll., *In preparation*, 1997.

[13] ALEPH coll., *CERN–PPE/97–003*, to be submitted to *Z. Phys. C*.

[14] Y.L Dokshitzer et al., *Basics of Perturbative QCD*, Editions Frontieres, 1991.

[15] S. Martí i García, *PhD Thesis*, Universitat de Valencia, 1996; hep–ex/9511004.

[16] DELPHI coll., *Nucl. Inst. and Meth. A* ***303*** (91) 233.

[17] DELPHI coll., *Nucl. Inst. and Meth. A* ***378*** (96) 57–100.

[18] S. Catani et al., *Phys. Lett. B* ***269*** (91) 432.

[19] M.L. Mangano and P. Nason, *Phys. Lett. B* ***285*** (92) 160.

[20] OPAL coll., *Phys. Lett. B* ***353*** (95) 595.

[21] DELPHI coll., *CERN–PPE/97–39*, submitted to *Phys. Lett. B*.

[22] DELPHI coll., *Z. Phys. C* ***65*** (95) 555.

[23] T. Sjöstrand, *Comp. Phys. Comm.* ***39*** (86) 346.

[24] P.V. Chliapnikov et al., *Phys. Lett. B* ***300*** (93) 183.

[25] P. Carruthers and C.C. Smith, *Int. Jour. of Modern Phys. A**5*** (87) 1447–1547.

[26] DELPHI coll., *Phys. Lett. B**347*** (95) 447.

[27] SLD coll., *Phys. Lett. B**385*** (96) 475.

[28] OPAL coll., *Z. Phys. C**69*** (96) 543.

[29] ALEPH coll., *Phys. Lett. B**384*** (96) 353.

[30] H.B. Nielsen Z. Koba and P.Olesen, *Nucl. Phys. B**40*** (72) 317.